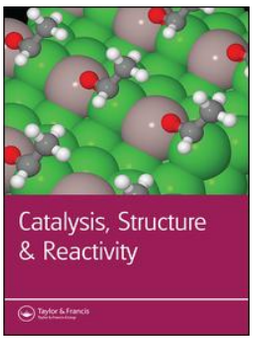

Catalysis, Structure & Reactivity

ISSN: 2055-074X (Print) 2055-0758 (Online) Journal homepage: https://www.tandfonline.com/loi/ycsr20

Application of work function measurements in the study of surface catalyzed reactions on Rh(1 0 0)

Basar Caglar, Ali Can Kizilkaya, J. W. (Hans) Niemantsverdriet & C. J. (Kees-Jan) Weststrate

To cite this article: Basar Caglar, Ali Can Kizilkaya, J. W. (Hans) Niemantsverdriet & C. J. (Kees-Jan) Weststrate (2018) Application of work function measurements in the study of surface catalyzed reactions on Rh(1 0 0), Catalysis, Structure & Reactivity, 4:1, 1-11, DOI: 10.1080/2055074X.2018.1434986

To link to this article: https://doi.org/10.1080/2055074X.2018.1434986

Published online: 12 Feb 2018.

CATALYSIS, STRUCTURE & REACTIVITY, 2018
VOL. 4, NO. 1, 1–11
https://doi.org/10.1080/2055074X.2018.1434986

Taylor & Francis
Taylor & Francis Group

Application of work function measurements in the study of surface catalyzed reactions on Rh(1 0 0)

Basar Caglar[a,c], Ali Can Kizilkaya[b,c], J. W. (Hans) Niemantsverdriet[c,d] and C. J. (Kees-Jan) Weststrate[d]

[a]Department of Energy Systems Engineering, Yasar University, Izmir, Turkey; [b]Department of Chemical Engineering, Izmir Institute of Technology, Izmir, Turkey; [c]Laboratory for Physical Chemistry of Surfaces, Eindhoven University of Technology, Eindhoven, The Netherlands; [d]Syncat@DIFFER, Syngaschem BV, Eindhoven, The Netherlands

ABSTRACT

The present article aims to show how work function measurements (WF) can be applied in the study of elementary surface reaction steps on metallic single crystal surfaces. The work function itself can in many cases not be interpreted directly, as it lacks direct information on structural and chemical nature of the surface and adsorbates, but it can be a powerful tool when used together with other surface science techniques which provide information on the chemical nature of the adsorbed species. We here, illustrate the usefulness of work function measurements using Rh(100) as our model catalyst. The examples presented include work function measurements during adsorption, surface reaction, and desorption of a variety of molecules relevant for heterogeneous catalysis. Surface coverage of adsorbates, isosteric heat of adsorption, and kinetic parameters for desorption, desorption/decomposition temperatures of surface species, different reaction regimes were determined by WF with the aid of other surface science techniques.

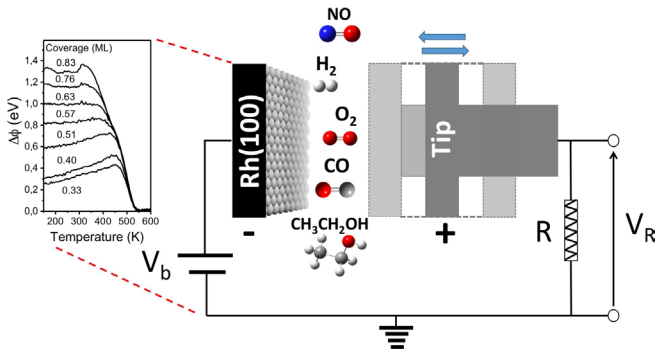

ARTICLE HISTORY
Received 13 October 2017
Accepted 26 January 2018

KEYWORDS
Work function; Kelvin probe; single crystal; adsorption; desorption; surface reaction; catalysis; spectroscopy

1. Introduction

Adsorption of the reactants forms the starting point of the catalytic cycle for chemical reactions catalyzed by solid surfaces. The catalyst surface provides a reactive platform that stabilizes the reactants and allows them to meet one another and react, after which the surface is regenerated by desorption of the reaction products. According to the Sabatier principle the optimal catalyst for a given process is a compromise: on the one hand the catalyst surface has to be sufficiently reactive to bind and activate reactants and reaction intermediates, but at the same time binding of the product should be weak enough so that product desorption can occur sufficiently fast. This sets the playing field for research that intends to better understand the intriguing phenomenon of catalysis: we need information about *kinetics*, describing the dynamics of adsorption, the rate of surface reactions and the desorption process. Kinetics are intimately related to *thermodynamics*: the barrier for desorption can in many cases be solely attributed to the adsorption energy, and for many elementary reactions a Brønsted-Evans-Polanyi relationship exists between the activation energy and the adsorption energies of either reactants or products.

CONTACT Basar Caglar basar.caglar@yasar.edu.tr

Experiments where single crystal surfaces with a well-defined structure are studied in a clean, well-controlled UHV environment are uniquely suited to study the kinetics and thermodynamics of a surface catalyzed reaction, as the high definition of the system allows us to study individual elementary processes in isolation. Fast, *in situ* measurement of the adsorbate concentration (θ_n) provides us a combination of θ_n and $d\theta_n/dt$ at different pressures and temperatures. In a simple Langmuir model the rate of adsorption and the rate of surface reaction for the general reaction $A_{ad} + B_{ad} \rightarrow C_{ad}$ are given as follows:

$$r_{\text{ads}} = \frac{d\theta_n}{\mathrm{d}t} = r_{\text{arrival}}\, S_0\, (1 - \theta_n) \tag{1}$$

$$r_{\text{Cform}} = \frac{d\theta_C}{\mathrm{d}t} = k\theta_A\theta_B \tag{2}$$

These formulas illustrate that the initial sticking coefficient can be determined when both θ_n and $d\theta_n/dt$ are known. Likewise, the reaction rate constant can be determined when both the rates and the reactant concentrations are known.

When the adsorption-desorption process is fully equilibrated the isosteric heat of adsorption of a reactant or product molecule, a thermodynamic property, can be determined by making use of the Clausius-Clapeyron Equation [1]:

$$\left(\frac{\partial ln(\frac{P_n}{P^o})}{\partial(\frac{1}{T})}\right)_{\theta n=constant} = -\frac{\Delta H_{\text{ads}}}{R} \tag{3}$$

In practice one determines a range of pressure-temperature combinations that produce the same coverage. The slope of $\ln(P_A/P_0)$ vs $1/T$ then provides the isosteric heat of adsorption. An accurate determination of surface coverage, preferably in a wide temperature and pressure regime, is thus required to obtain good estimate of ΔH_{ads}.

For desorption processes the transient mass signal of the desorbing species directly provides $d\theta_n/dt$, and θ_n can then simply obtained by integration of the signal. Likewise, reactions that produce a gaseous product, e.g. CO oxidation to produce CO_2, can be easily followed by mass spectrometer. But for many other processes, e.g. low temperature decomposition steps of hydrocarbon species or oxygenates [2], or for high temperature reactions where high reactant pressures are used, e.g. water formation and CO_2 formation on reactive metals such as cobalt and ruthenium other *in situ* tools are needed.

The work function of a single crystal sample is affected by the outermost layer of the sample, and changes on the surface induce a change of the work function that can easily be measured with high resolution in a matter of seconds using a Kelvin probe. Since the technique does not require vacuum to work it can be employed at relatively high reactant pressures and high surface temperatures [3–9]. Most adsorbates affect the work function (Φ) and their concentration can be deduced from the work function change ($\Delta\Phi$). This technique is thus ideally suited to determine both θ_n and $d\theta_n/dt$ *in situ*, which is particularly useful for the study of surface reactions that do not instantaneously produce gaseous species or that require high reactant pressures to proceed.

In this article we discuss how work function measurements by means of a Kelvin probe can be used to study the elementary steps of a surface-catalyzed reaction such as adsorption, surface reaction and desorption. The examples we provide here were measured on a Rh(1 0 0) surface for which many reference data are available so that the results observed work function changes can be interpreted in detail. We refer to the supplementary information for a more detailed discussion about the working principle of the Kelvin probe and on the origin of surface sensitivity of the work function.

2. Experimental

The experiments were performed in a home-built UHV chamber with a base pressure $\leq 3 \times 10^{-10}$ mbar. Pressures in both chambers were measured using a cold cathode gauge (ActiveLine PKR251). A typical cleaning cycle consists of sputter-annealing cycles followed by oxygen treatment to remove surface carbon, described in detail elsewhere [10]. A UHV Kelvin probe (UHV KP 4.5, KP Technology) was used to measure $\Delta\Phi$. It consists of a stainless steel disc which is suspended parallel to the Rh(1 0 0) crystal to form a simple capacitor (Figure 1(b)). The oxide layer on the stainless steel tip makes it comparatively inert for adsorption of reactants such as CO. For example, CO desorption from chromium oxide, one of the oxides expected to be present at a stainless steel surface, occurs around 180 K already [11]. As the tip is kept at room temperature throughout the experiments CO adsorption on the tip is negligible. In general, no indications were found throughout the experiments presented here as well as elsewhere [2–5] that the work function measurement was affected by a change of the work function of the tip.

The $\Delta\Phi$ between two samples is then determined by vibrating the KP tip and adjusting the back potential (V_b, see Figure 2(b)) until it equals $\Delta\Phi$ between the sample and tip. As Φ_{tip} remains constant throughout the experiment the measured $\Delta\Phi$ can be attributed to a change of the work function of the Rh(1 0 0) sample. All work function data reported here is with respect to the clean

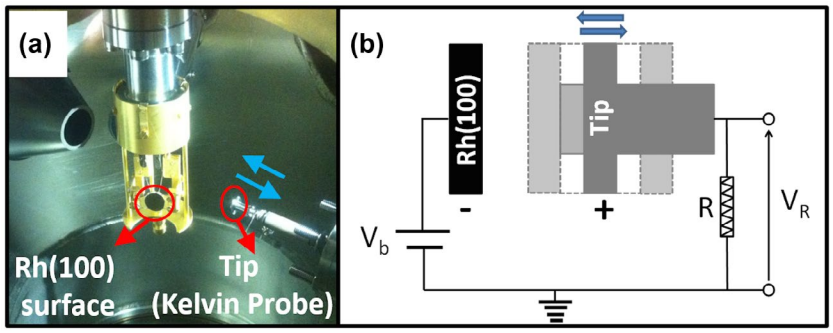

Figure 1. (a) Picture of the Rh(100) single crystal and the tip of the UHV-compatible Kelvin probe. (b) Simplified circuit diagram of the Kelvin probe.

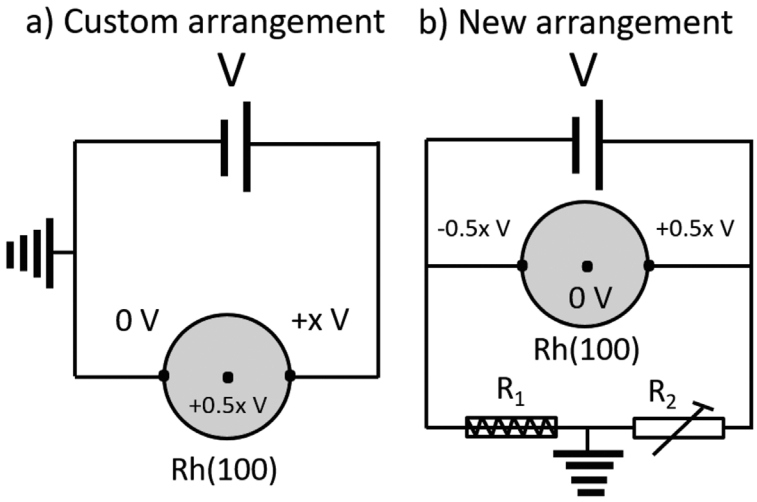

Figure 2. Simplified circuit diagram for the resistive heating: (a) Custom arrangement with one side of the Rh(100) single crystal connected to ground potential. (b) Improved arrangement, with the crystal center at ground potential due to the variable resistor bridge used.

Rh(1 0 0) surface. Although the absolute work function is of little value for the present study it can be computed easily from the reported data by adding the value for clean Rh(1 0 0), 5.1 eV, which has been reported previously [11,12]).

In order to minimize the effect of potential gradients across the sample during resistive heating the sample was grounded via an adjustable resistor bridge so that the center of the sample is approximately at zero bias (Figure 2(b)). In practice, one of the resistors was adjusted such that a minimal offset of the work function was found during heating. With the aid of this arrangement, measurements were carried out with an accuracy of ± 0.05 eV.

The reactants H_2, NO, CO and ethene were used without further purification. Oxygen was dosed in the form of synthetic air, 20% O_2 in N_2, and ethanol (99.8%, Merck) was degassed by repeated freeze-pump-thaw cycles before use. Adsorption was typically done with the sample held at 100–150 K. For temperature programmed experiments a heating rate of 1 Ks^{-1} was used. In many cases both ΔΦ and gas phase products were measured in a single temperature ramp.

3. Results and discussion

In the first part of our study we establish the relation between ΔΦ and adsorbate coverage for a variety of atomic and molecular adsorbates. We then use this information to measure the equilibrium value of θ_{CO} at various CO pressures and surface temperatures to derive the isosteric heat of adsorption of CO. In the last part we discuss how surface reactions can be probed using work function measurements. The kinetics of CO desorption are followed by determining θ_{CO} during heating of a CO_{ads} layer in vacuum. This data-set is then used to determine the activation energy and pre-exponential factor for desorption. Finally, work function measurements for CO oxidation, NO dissociation and ethanol decomposition are presented and discussed in relation to the available knowledge about the thermal evolution of these systems.

3.1. Adsorption via work function measurements

Since the work function is not always linearly dependent on adsorbate concentration temperature programmed desorption (TPD) and temperature programmed

reaction spectroscopy (TPRS) experiments were used to establish the relation between ΔΦ and surface coverage, for the atomic adsorbates H_{ad}, O_{ad}, C_{ad}, and the molecular adsorbates CO_{ad}, and $CH_3CH_2O_{ad}$. Carbon was deposited by decomposing ethylene and the coverage was derived from the H_2 formed in the process [13]. Ethoxy species ($CH_3CH_2O_{ad}$) form upon ethanol adsorption on Rh(1 0 0), and the hydrogen produced remains adsorbed as well [14]. Since H_{ad} produces only a very small ΔΦ the observed work function change can be practically completely attributed to adsorbed ethoxy species.

Figure 3 shows ΔΦ as a function of adsorbate coverage (from 0 to saturation coverage) for different adsorbates. The work function decreases with coverage for ethoxy suggesting that it creates a positive outward dipole layer. Conversely, CO, atomic oxygen, carbon and hydrogen cause an increase of the work function due to their negative outward dipole layer.

For CO_{ad} we find a ΔΦ of 1.35 eV for the saturation coverage of CO (0.83 ML). The work function change as function of CO coverage shows two different regimes: the slope of the curve for $\theta_{CO} < 0.4$ ML is smaller than that for $\theta_{CO} > 0.4$ ML, consistent with earlier literature reports [11]. The increase of the slope above 0.4 ML can be assigned to the change in the site occupancy of CO. For $\theta_{CO} < 0.5$ ML CO occupies top sites, ultimately forming a well-ordered $c(2 \times 2)$ structure when $\theta_{CO} = 0.5$ ML. Above 0.5 ML a transition from the $c(2 \times 2)$ into a more condensed $p(4\sqrt{2} \times \sqrt{2})R45°$ structure occurs, which results in an increase in the amount of bridge bonded CO [15,16]. The higher electron back-donation from the metal surface for CO_{bridge} compared to CO_{top} causes a larger ΔΦ for CO_{ad} in the bridge position. An alternative explanation has been proposed for CO on the Ni(1 0 0) surface, where the larger ΔΦ at high coverage is attributed to increased CO–CO repulsion in the compressed adlayer [17].

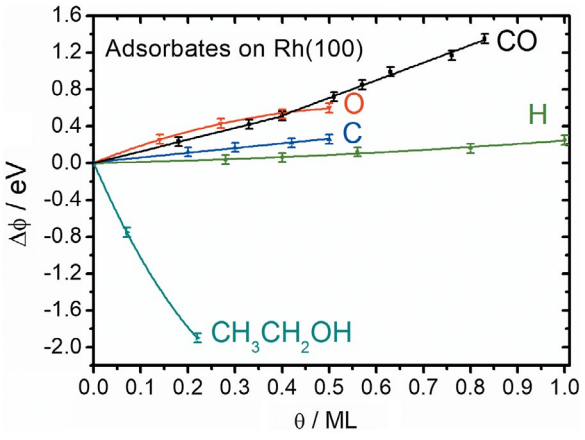

Figure 3. Work function change upon adsorption of different species as a function of coverage. The error margin is ± 0.05 eV for all measurements, based on the noise level of the instrument.

The adsorption of atomic oxygen, hydrogen and carbon creates a negative outward dipole layer due to their higher electronegativities compared to that of Rh metal. In other words, electron transfer occurs from the Rh(1 0 0) surface to the adsorbed atomic layer. Since the electronegativity of oxygen is the highest among them, ΔΦ upon oxygen adsorption is larger compared to atomic hydrogen and atomic carbon. The work function increases linearly with oxygen coverage and levels off near saturation (0.5 ML). Oxygen atoms occupy the fourfold hollow sites up to 0.4 ML [18,19], above which they occupy threefold sites due to the (2 × 2)-p4 g reconstruction [18,20,21]. The binding of oxygen on the threefold hollow site of the reconstructed surface near saturation could be the reason for lower ΔΦ. The same trend, i.e. a leveling off in ΔΦ as a function of oxygen coverage, was also observed on Au(1 1 1) where ozone was used as a source of atomic oxygen. In this case Saliba et al. [22] propose that mutual depolarization of oxygen atoms causes this leveling off.

The ΔΦ due to surface carbon shows a linear increase with surface coverage, consistent with the Helmholtz equation [23–25], indicating that there is no significant change in the chemical nature of the ad-layer such as a different bonding site or the formation of carbide. Since H_{ad} occupies fourfold hollow sites at all coverages [11,26,27] and subsurface adsorption of hydrogen is not feasible due to the low stability of bulk rhodium hydride [28,29] we also expect a linear correlation between ΔΦ on the hydrogen surface coverage. Since hydrogen produces a ΔΦ of only 0.25 eV at 1 ML coverage the apparent slight deviation from linearity that can be seen in Figure 3 should most likely be attributed to the relatively low precision of the measurements. Therefore, we feel that further interpretation of this effect is not warranted.

Ethanol decomposes to ethoxy upon adsorption, which causes a decrease of the work function. This can be explained by the orientation of the ethoxy adsorbate, which binds with the oxygen (negative) end bonding to the surface and the hydrocarbon end (positive) pointing away from the surface [14].

3.2. Adsorption/desorption equilibrium

The adsorption-desorption equilibrium of CO on Rh(1 0 0) was studied to determine the isosteric heat of adsorption (or desorption energy since there is no additional barrier for CO desorption). To this end, the previously established relation between ΔΦ and θ_{CO} was used to derive the CO coverage at different combinations of CO pressure and surface temperature. Figure 4(a) shows a number of adsorption isotherms, recorded at the surface temperatures indicated in the figure.

These isotherms deviate from a simple Langmuir adsorption isotherm. This can be explained by the presence of adsorption sites with different stabilities and lateral interactions. CO adsorbed on bridge site is known

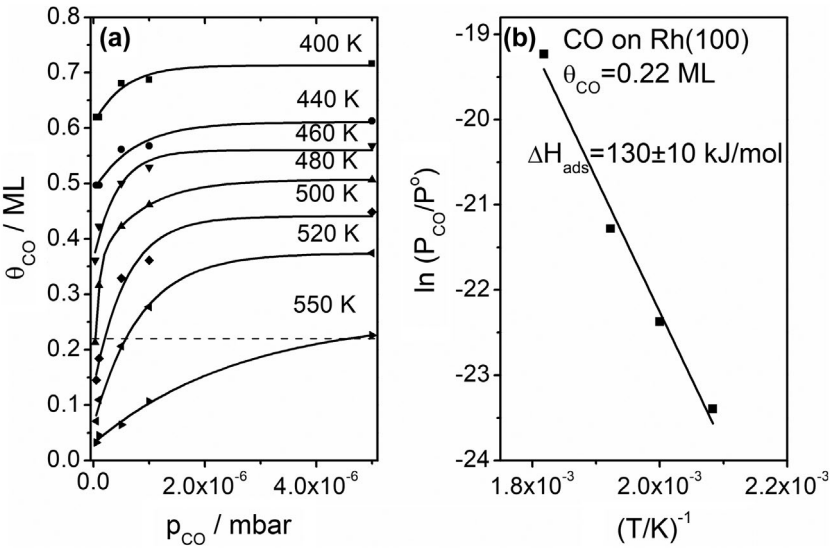

Figure 4. (a) Adsorption isotherms of CO at different temperatures measured with work function change. (b) Adsorption isostere of CO on Rh(100). The slope equals −ΔH/R.

to be less stable than CO on top sites [15,30] and the lateral interaction of CO molecules was determined to be 9–24 kJ/mol via Monte-Carlo simulations [31,32].

These adsorption isotherms can be used to derive the adsorption energy (enthalpy of adsorption) of CO on Rh(1 0 0) surface for a given CO coverage by using the Clausius-Clapeyron equation (Equation (3)). Figure 4(b) shows a plot of $\ln(P/P_0)$ vs $1/T$, for $\theta_{CO} = 0.22$ ML. From the slope, $-\Delta H/R$, we find a CO adsorption energy of 130 ± 10 kJ mol^{-1}. The result is consistent with the one obtained via TPD experiments for the same coverage (125 kJ/mol) [33]. In these experiments the main uncertainty is introduced by the difficulty to determine the exact reactant pressure in the UHV regime. In addition to this, the shielding effect due to the close proximity of the Kelvin probe tip to the sample surface can lower the effective pressure over the sample surface [2]. However, as long as these deviations scale linearly with pressure small inaccuracies in the exact pressure measurement only affect the offset of the $\ln(P/P_0)$ vs $1/T$ plot, and therefore do not affect the value of ΔH that is calculated from the slope.

3.3. Work function measurements to determine reaction kinetics: CO desorption

As ΔΦ measurements take only a few seconds θ_n can be determined *in situ*, *during* heating, and and $d\theta_n/dt$ can be determined from time derivative of θ_n. This information can be used for a kinetic analysis to determine the kinetic parameters. We illustrate this by looking at a very simple reaction, the desorption of CO from the surface, for which we can simultaneously measure the desorption using a mass spectrometer. The work function measurements obtained during heating for different initial CO coverages are shown in Figure 5, along with the corresponding desorption spectra. The initial CO coverage reported in the figure was determined by integration of the desorption peak area (5b). The work function drops to the clean surface value for $T > 550$ K, indicating that all CO has desorbed molecularly and CO bond scission, which would produce C_{ad} and O_{ad} can be excluded.

At a $\theta_{CO} < 0.6$ ML the work function shows a small increase with temperature until CO desorbs. This is attributed to continued CO adsorption on the sub-saturated surface due to slow pumping out of the UHV chamber after dosing CO. This additional CO is included in the quantification, since the coverages reported in the figure have been determined by integration of TPD peak area.

At a coverage close to saturation point of 0.83 ML the work function shows a 0.1 eV increase around 300 K, concurrent with a small CO desorption peak as seen by the mass spectrometer at this temperature. This desorption peak is assigned to the transition from the c (6 × 2) structure (0.83 ML) to a p (4√2 × √2)R45° (0.75 ML) structure. In the c (6 × 2) structure, CO mainly occupies top sites whereas in the p (4√2 × √2)R45° structure CO occupies both top and bridge sites. The transition from the former to the latter occurs due to CO desorption [34], and the increase in Φ around this temperature is assigned to the combined effect of change in site occupancy of CO molecules and CO desorption.

The kinetic parameters for CO desorption for different coverages were determined using the coverage-corrected leading-edge analysis, which is based on linearization of the Arrhenius equation (Equation (4)) over a small interval at the low-temperature side of the spectrum where the decrease in coverage is negligible. This method gives a higher accuracy of the kinetic parameters over a larger temperature interval [35].

$$\ln\left(\frac{r_{des}}{\theta^n}\right) = \ln\left(k_{des}\right) = \ln(\nu_{des}(\theta)) - \frac{E_{des}(\theta)}{RT} \quad (4)$$

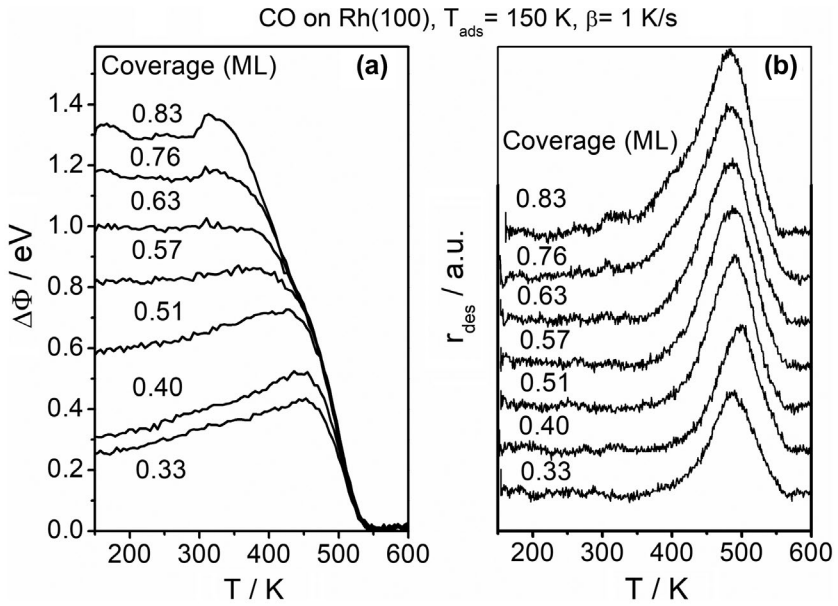

Figure 5. (a) Work function change during CO desorption for different CO coverage and. (b) the corresponding CO (m/e = 28) desorption spectra. Both ΔΦ and m/z = 28 were recorded in a single experiment using a heating rate of 1 K s^{-1}. The work function was measured for every 5s.

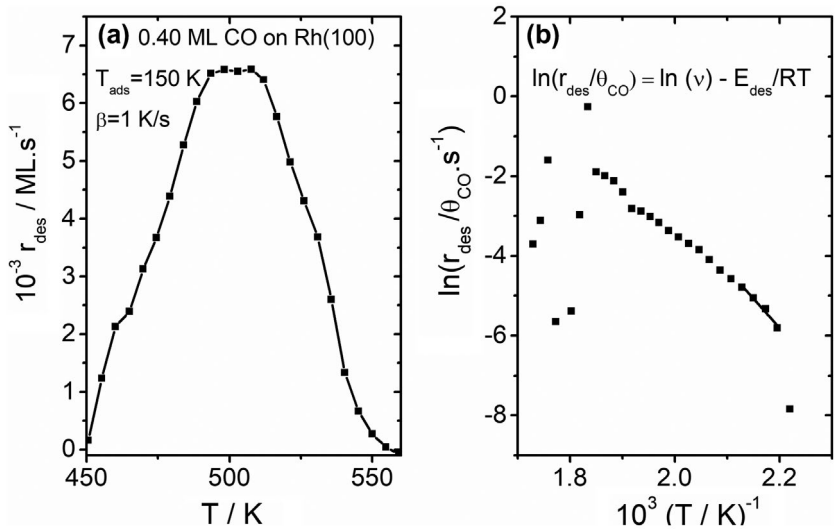

Figure 6. (a) calculated CO desorption rate as a function of temperature obtained from work function measurement for 0.40 ML CO desorption. (b) $\ln(r_{des}/\theta_{CO})$ vs 1/T plot to derive the activation energy and pre-exponential factor for CO desorption.

(r_{des} is desorption rate, k_{des} is the rate constant for desorption, n is the reaction order, v_{des} is the pre-exponential factor and E_{des} is the activation energy)

After converting the work function data to CO coverage the desorption rate, $r_{des} = -\frac{d\theta_{CO}}{dt}$ was obtained by taking the time derivative of the CO coverage, shown in Figure 6(a) for an initial CO coverage of 0.40 ML. As expected, the resulting spectrum is similar to the corresponding TPD spectra in terms of peak shape and peak temperature. The activation energy and pre-exponential factor were determined as 120 ± 5 kJ mol^{-1} and $10^{11.5 \pm 0.5}$ s^{-1} from the slope and intercept of the line at low temperature side from a plot of the natural logarithm of the CO desorption rate divided by the CO coverage against the reciprocal temperature (Figure 6(b)). In order to minimize the effect of the uncertainty in the measured work function on the natural logarithm of the desorption rate divided by coverage term and the resulting activation energy and pre-exponential factor, we have only used set of data at the low temperature-side of the plot where coverage change is negligible. The calculated activation energy and pre-exponential factor are consistent with the literature for a coverage of 0.40 ML (E_{des} = 115 kJ mol^{-1} and $v = 10^{11.7}$ s^{-1}) [33].

3.4. Monitoring surface reactions

Several surface reactions were investigated by work function measurements. The changes on the surface were studied during CO oxidation, decomposition of

nitric oxide and ethanol decomposition. Since the reaction products in the last two cases do not always leave the surface instantly these examples illustrate the particular usefulness of *in situ* ΔΦ measurements alongside mass spectrometer measurements of the gas phase to analyze the kinetics for such cases.

3.4.1. CO oxidation

First the effect of pre-adsorbed oxygen on CO adsorption was investigated by work function measurements. After dosing O_2 to the surface held at 150 K to obtain the amounts of O_{ad} indicated in Figure 7 CO was then dosed to the surface and the work function was recorded. To obtain the absolute CO coverage plotted in Figure 7 the coverages of the pre-adsorbed oxygen and CO were determined via integration of the CO_2 and CO peak areas from TPRS. Figure 7 shows ΔΦ upon CO exposure to the oxygen-free and oxygen-covered surfaces. The data in the inset shows how ΔΦ changes due to the presence of the O_{ad}. In the main panel these initial ΔΦ values were subtracted from the ΔΦ measured after dosing CO, to facilitate comparison and highlight the contribution of CO to the observed work function change. We find that the slope of ΔΦ as a function of θ_{CO} for *low* CO coverages on the oxygen-covered surface is identical to the slope found for *high* coverages, $\theta_{CO} > 0.4$ ML, on the oxygen-free surface. This is attributed to CO occupying mainly bridge and three/fourfold hollow sites on the oxygen covered Rh(1 0 0), compared to top and bridge sites on Rh(1 0 0). On oxygen-covered surfaces the slope of ΔΦ vs θ_{CO} levels off near the CO saturation point, most probably originating from the repulsive lateral interactions between CO and oxygen neighbors, which reduce back donation into CO molecules and changes the dipole moment of the CO molecules [19].

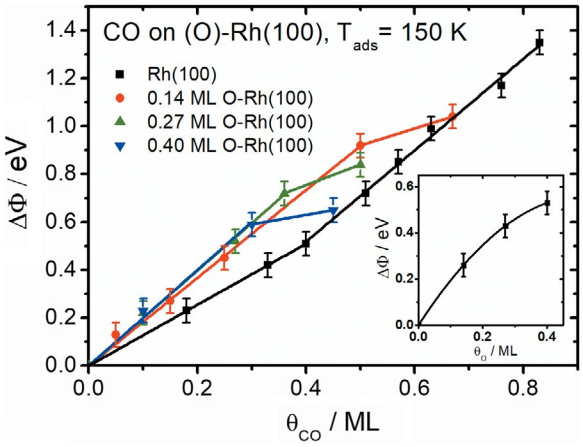

Figure 7. Work function change as a function of CO coverage for various amounts of oxygen pre-adsorbed surfaces. The inset shows the relative work function as a function of the pre-adsorbed oxygen concentration before dosing CO. The error margin is ±0.05 eV for all measurements, based on the noise level of the instrument.

Figure 8(a) shows the ΔΦ data as a function of temperature during heating of after post-dosing CO onto 0.14 ML O_{ad}. Figure 8(b) shows the corresponding CO (m/z = 28) and CO_2 (m/z = 44) desorption traces detected by the mass spectrometer. Here the the clean Rh(1 0 0) surface was again used as reference point, and the initial ΔΦ values are due to the combined influence of O_{ad} and CO_{ad}. For the lowest CO coverage used here, 0.05 ML the mass spectrometer data shows that all CO is oxidized to CO_2 around 430 K. The loss of both CO_{ad} and O_{ad} causes a decrease of the work function at the same temperature. Since O_{ad} was present in excess the work function does not return to the clean surface value. Instead, by using the correlation between ΔΦ and θ_O established earlier we find an O_{ad}-coverage of 0.08 ML for T > 450 K, in good agreement with the stoichiometry of the reaction (0.14 ML−0.05 ML = 0.09 ML).

For all other CO coverages all the surface oxygen is consumed and a ΔΦ equal to the clean surface value is found for T > 550 K. An increase of the CO coverage leads to a downward shift of the CO_2 formation temperature and an increase of the quantity of unreacted CO that desorbs around 500 K.

Four different CO oxidation regimes have previously been identified on the (1 0 0) facet of Rhodium [19,36]. By taking the time derivative of ΔΦ (Figure 9) the work function data can be more easily compared to the TPD spectra. The information obtained from both ΔΦ and TPD is similar: at a CO coverage above 0.5 ML the peaks in $\Delta\Phi/dt$ located at 270 and 350 K are assigned to CO_2 formation, whereas the peak at 500 K is due to desorption of the excess CO_{ad}. For CO coverages below 0.5 ML CO_2 formation occurs around 430 K. According to literature these three CO_2 formation peaks can be attributed to the following reactions [19,36]: (i) The peak at 270 K is assigned to CO reacting with one of the three neighboring oxygen atoms in ac (2 × 2) ordering; (ii) the peak at 350 K is attributed to the reaction between CO on bridge site and oxygen in a p (2 × 2) ordering; (iii) the peak at 430 K reflects low reactivity between oxygen and CO.

3.4.2. NO dissociation

Decomposition of NO produces O_{ad} and N_{ad}, which both affect the work function. The decomposition of NO can thus be studied *in situ* using a Kelvin probe. Figure 10 shows ΔΦ and the corresponding m/z = 28 (N_2) and m/z = 30 (NO) mass signals during heating of an NO-saturated surface (0.65 ML,[37]) in vacuum. The saturation coverage of NO adsorption produces a 0.9 eV increase in ϕ, due to negative outward dipole layer of NO, in agreement with the literature value of 0.93 eV [38]. The work function decreases sharply at 420 K, which is attributed to both NO desorption and NO decomposition. The observed temperature (420 K) for NO decomposition is in good agreement with the literature (425 K) [37].

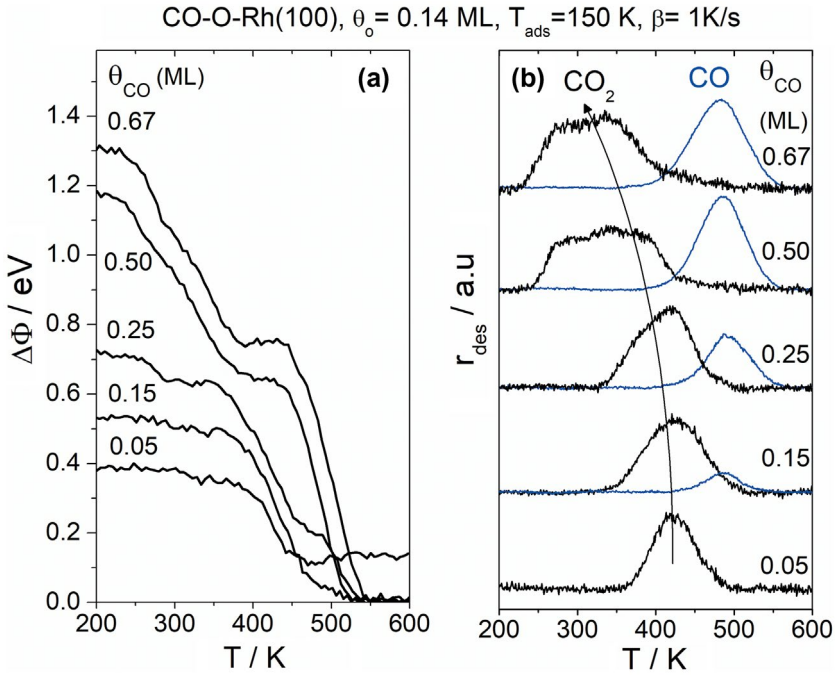

Figure 8. (a) Work function change during CO oxidation for different coverage of CO on 0.14 ML oxygen pre-covered surface. (b) CO and CO_2 desorption spectra obtained after CO oxidation.

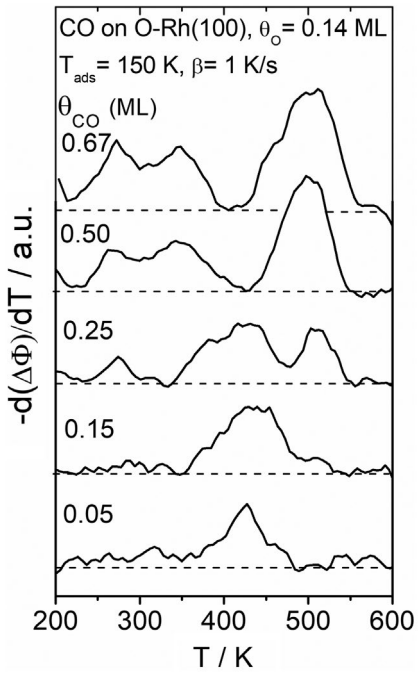

Figure 9. The rate of work function change during CO oxidation for different coverage of CO on 0.14 ML oxygen pre-covered surface.

The resulting nitrogen atoms recombine and desorb as N_2 at 700 K, causing further ~0.1 eV decrease of the work function and leaving only atomic oxygen on the surface. The work function after N_2 desorption is still 0.52 eV higher than the clean surface value, which translates to a θ_O of 0.37 ML (see Figure 3), i.e. 0.37 ML of the initial 0.65 ML NO_{ad} present dissociates. This value in excellent agreement with an earlier TPD study of NO dissociation on Rh(1 0 0), in which quantitative analysis of the N_2 formed indicates that 0.37 ML NO decomposes [37].

3.4.3. *Ethanol decomposition*

Our previous work showed that adsorbed ethoxy ($+H_{ad}$) forms upon ethanol adsorption on Rh(1 0 0). These ethoxy species decompose < 200 K already and the H_{ad}, CH_{xad} and CO_{ad} species produced remain adsorbed on the surface [14]. This means that this decomposition step cannot be probed by a TPD experiment. Here we explore how work function measurements can be used to study this surface reaction that occurs at low temperature. Figure 11 shows both ΔΦ and the gas phase products formed during heating after dosing a low (0.07 ML) and a high (0.22 ML) quantity of ethanol to the surface. As mentioned earlier, ethoxy adsorbates produce a strong decrease of the work function. For the low coverage experiment the work function changes around 190 K, from −0.75 eV to + 0.3 eV. Since the mass spectrometer does not detect any desorbing products (e.g. molecular ethanol) the change must be due to a change of the chemical nature of the adsorbate layer. Indeed, our previously published RAIRS data indicates that ethoxy decomposes around 200 K to CO_{ad}, H_{ad} and CH_x, species that cause a positive rather than a negative work function change with respect to the clean surface (see Figure 3). The work function then decreases around 300 K, which can be attributed to the loss of H_{ad}, evident from the concurrent H_2 desorption peak. The decrease of 0.09 eV corresponds to a hydrogen coverage of 0.4 ML close to the maximum possible quantity of 0.42 ML (0.07 × 6). The slight work function increase between 350–450 K is most likely due to a rearrangement of the

surface adsorbates, possibly involving a small quantity of CH_x species. CO desorption occurs around 490 K, which amounts to 0.07 ML according to analysis of the desorption peak area. Interestingly, the work function change at this point amounts to −0.23 eV. According to the data reported in Figure 3 this would correspond to as much as 0.18 ML CO_{top}. This discrepancy between MS-based quantification and quantification based on work function measurements shows that C_{ad} strongly affects the magnitude of the CO-induced work function shift, making quantitative interpretation of the work function data for this co-adsorption system difficult. TPD indicates that only surface carbon is left after heating to 550 K. The ΔΦ of 0.04 eV at this point translates to a carbon coverage of ~0.07 ML C_{ad}, in good agreement with quantification based on TPD and TPO [14].

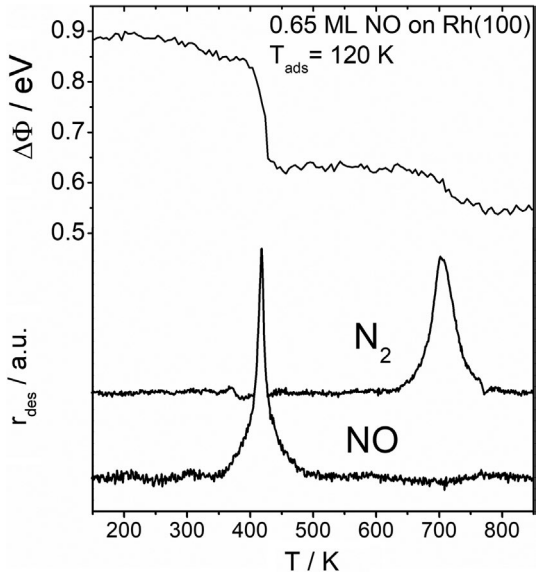

Figure 10. Temperature programmed work function measurement and $m/z = 28$ (N_2) and $m/z = 30$ (NO) desorption traces obtained after saturation coverage (0.65 ML) NO adsorption at 120 K and subsequent heating to 850 K with a rate of 1 K s^{-1}.

For the high coverage the strong increase of the work function is found at the same temperature ~190 K, showing that the ethoxy decomposition temperature is independent of the ethoxy coverage. Since multiple processes contribute to the work function changes seen between 200–400 K, i.e. molecular ethanol desorption, methane formation and H_2 desorption, quantitative interpretation is difficult. We here limit the analysis to quantification of the surface carbon formed. The ΔΦ of 0.09 eV at the end of the experiment corresponds to 0.18 ML carbon. The 0.02 ML difference between the 0.20 ML of ethanol decomposed (derived from the amount of CO produced) and the 0.18 ML C_{ad} found afterwards (by both TPO and ΔΦ) can be attributed to the formation of methane (see Ref. [14]).

3.5. Advantages and disadvantages of work function measurements

Work function measurements have several advantages over other surface science techniques in the study of surface catalyzed reactions. Work function measurements provide faster way than TPD to determine surface coverage and kinetic parameters of desorption once the correlation between adsorbate coverage and work function change is set. Moreover, the coverage of surface species left after surface reaction such as surface carbon

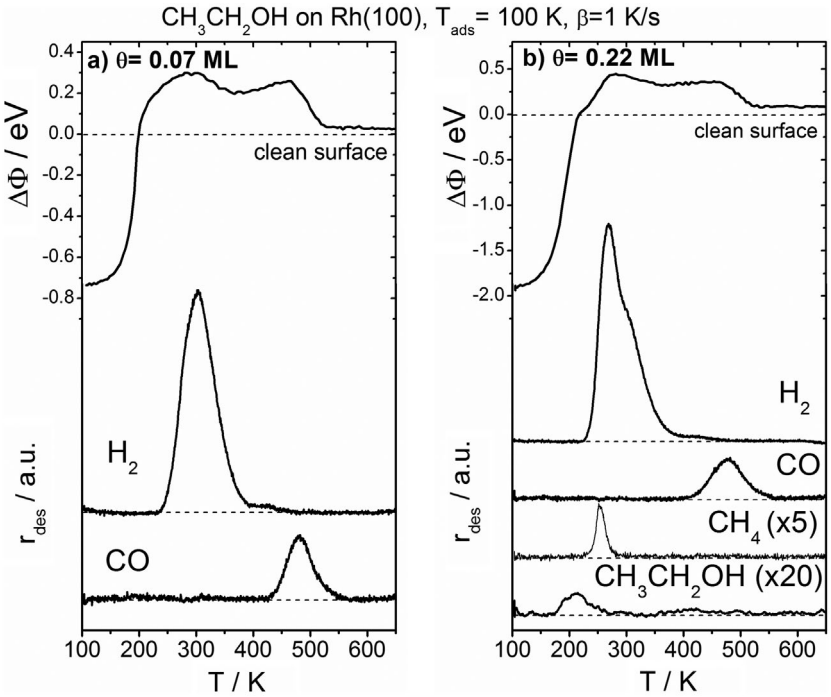

Figure 11. Temperature programmed work function measurement and TPD spectra obtained after 0.07 ML (a) and 0.22 ML (b) ethanol adsorption at 100 K and subsequent annealing to 650 K.

and oxygen can be found easily by using work function measurement without the need of an additional experiment, as opposed to TPD analysis.

Work function measurements are not limited by reactant pressure unlike techniques such as XPS, EELS and LEED. Thus, it is relatively easy to determine the isosteric heat of adsorption from equilibrium measurements using pressures incompatible with electron-bases spectroscopies. One of the other advantage of work function measurements over other surface science techniques such as RAIRS, EELS and XPS is that the technique possesses a high time resolution in terms of monitoring surface reaction, or more specifically decomposition temperatures.

The main disadvantage of the technique is that it only provides indirect information, as the work function is sensitive to both structure and adsorbate concentrations. Additional experimental techniques are therefore needed, such as LEED, XPS, SIMS, TPRS and RAIRS for interpreting results. Moreover, if more than one surface event (e.g. desorption, surface site rearrangements) happens simultaneously (e.g. desorption and surface reconstruction), it is difficult to identify the individual contribution of each phenomenon to the work function change.

4. Conclusions

We have tested the ability of work function measurements as a surface science tool for the study of the elementary steps of surface-catalyzed reactions such as adsorption, surface reaction and desorption. We present some illustrative examples on Rh(1 0 0), which serves as a representation for other metal surfaces. The link between surface coverage and work function change was explored for CO_{ad}, O_{ad}, H_{ad}, C_{ad} and ethoxy on Rh(1 0 0). For adsorbates such as C_{ad}, H_{ad} and ethoxy we find a simple linear correlation between coverage and work function change, whereas for CO_{ad} and O_{ad} a more complex correlation was found. In particular for CO_{ad} it was found that co-adsorbates such as O_{ad} and C_{ad} influence the CO-induced work function change significantly.

The isosteric heat of adsorption for CO was determined by measuring a large number of adsorption isotherms at different surface temperatures and CO pressures up to ~10^{-5} mbar. This experiment illustrates that work function measurements are compatible with high reactant pressures [4]. Combined with short measurement times this makes it possible to measure a large number of isotherms (and/or isobars) from which the isosteric plot of $\ln(P/P_0)$ vs 1/T can be constructed to determine ΔH [5]. Fast, *in situ* measurement of θ_{CO} also makes it possible to follow relatively fast surface processes, such as CO desorption during heating of the surface. The data can then be used to derive the kinetic parameters using a method that is practically identical to the analysis of TPD data.

For surface reactions the combination of work function measurements, which probes the surface composition, with a mass spectrometer to probe the nature and concentration of gaseous reaction products, proves to be particularly powerful to get a complete picture of the reaction. In the example of CO oxidation presented here the mass spectrometer can distinguish between desorption of unreacted CO vs formation of CO_2. The disappearance of CO is also evident from the work function measurements, but these measurements also give information on the situation after reaction: for a low CO coverage O_{ad} is left behind and this is easily detected by the work function measurement. Work function measurements are particularly important when products of a surface reaction do not desorb upon formation. We show that the NO decomposition reaction, which produces $N_{ad} + O_{ad}$, can be followed *in situ*. For ethanol decomposition work function measurements allow us to determine the exact temperature at which ethoxy adsorbates decompose to CO, H_{ad} and CH_x, with a time resolution that is difficult to obtain with many other surface science techniques. In conclusion, this simple and affordable, yet powerful experimental technique deserves a prominent place in the toolbox of scientists interested in studying surface reactions *in situ*.

Acknowledgement

We gratefully acknowledge Dutch National Research School Combination Catalysis Controlled by Chemical Design (NRSC-Catalysis) for funding of this research. Syngaschem BV acknowledges funding from Synfuels China Technology Co., Ltd, Beijing-Huairou, China.

Disclosure statement

No potential conflict of interest was reported by the authors.

Funding

This work was supported by Dutch National Research School Combination Catalysis Controlled by Chemical Design (NRSC-Catalysis); Synfuels China Technology Co., Ltd, Beijing-Huairou, China.

ORCID

Basar Caglar http://orcid.org/0000-0001-8732-6772
Ali Can Kizilkaya http://orcid.org/0000-0003-0623-648X
C. J. (Kees-Jan) Weststrate http://orcid.org/0000-0003-4346-166X

References

[1] Cengel Y, Boles MA. Thermodynamics: an engineering approach. Boston, (MA): McGraw-Hill; 2004.
[2] Weststrate CJ, Ciobîcă IM, van de Loosdrecht J, et al. Adsorption and decomposition of ethene and propene on Co(0 0 0 1): the surface chemistry of fischer-

tropsch chain growth intermediates. J Phys Chem C. 2016;120:29210–29224.
[3] Kizilkaya AC, Niemantsverdriet JW, Weststrate CJ. Oxygen adsorption and water formation on Co(0001). J Phys Chem C. 2016;120:4833–4842.
[4] Weststrate CJ, van Helden P, van de Loosdrecht J, et al. Elementary steps in fischer-tropsch synthesis: CO bond scission, CO oxidation and surface carbiding on Co(0001). Surf Sci. 2016;648:60–66.
[5] Weststrate CJ, van de Loosdrecht J, Niemantsverdriet JW. Spectroscopic insights into cobalt-catalyzed fischer-tropsch synthesis: a review of the carbon monoxide interaction with single crystalline surfaces of cobalt. J Catal. 2016;342:1–16.
[6] Koch MH, Jakob P, Menzel D. The influence of steps on the water-formation reaction on Ru(001). Surf Sci. 1996;367:293–306.
[7] Heras JM, Papp H, Spiess W. Face specificity of the H2O adsorption and decomposition on co surfaces - a LEED, UPS, sp and TPD study. Surf Sci. 1982;117:590–604.
[8] Papp H. Chemisorption and reactivity of carbon monoxide on a Co(0001) single crystal surface; studied by LEED, UPS, EELS, AES and work function measurements. Surf Sci. 1983;129:205–218.
[9] Papp H. Chemisorption and reactivity of carbon monoxide on a Co(1120) single crystal surface; studied by LEED, UPS, EELS, AES and work function measurements. Surf Sci. 1985;149:460–470.
[10] Caglar B, Niemantsverdriet JW, Weststrate CJ. Modeling the surface chemistry of biomass model compounds on oxygen-covered Rh(100). Phys Chem Chem Phys. 2016;18:23888–23903.
[11] Peebles DE, Peebles HC, White JM. Electron spectroscopic study of the interaction of coadsorbed CO and D2 on Rh(100) at low temperature. Surf Sci. 1984;136:463–487.
[12] Nieskens DLS, Ferre DC, Niemantsverdriet JW. The influence of promoters and poisons on carbon monoxide adsorption on Rh(100): a DFT study. Chem Phys Chem. 2005;6:1293–1298.
[13] Nieskens DLS, van Bavel AP, Ferre DC, et al. Ethylene decomposition on Rh(100): theory and experiment. J Phys Chem B. 2004;108:14541–14548.
[14] Caglar B, Olus Ozbek M, Niemantsverdriet JW, Weststrate CJ. The effect of C-OH functionality on the surface chemistry of biomass-derived molecules: ethanol chemistry on Rh(100). Phys Chem Chem Phys. 2016;18:30117–30127.
[15] Jansen MMM, Scheijen FJE, Ashley J, et al. Adsorption/desorption studies of CO on a rhodium(100) surface under UHV conditions: a comparative study using XPS, RAIRS, and SSIMS. Catal Today. 2010;154:53–60.
[16] de Jong AM, Niemantsverdriet JW. The adsorption of CO on Rh(100) – reflection absorption infrared spectroscopy, low-energy-electron diffraction, and thermal-desorption spectroscopy. J Chem Phys. 1994;101:10126–10133.
[17] Koel BE, Peebles DE, White JM. Low temperature coadsorption of hydrogen and carbon monoxide on Ni(100): I. TPD, Δ, and UPS studies. Surf Sci. 1983;125:709–738.
[18] Oed W, Dotsch B, Hammer L, et al. A leed investigation of clean and oxygen covered Rh(100). Surf Sci. 1988;207:55–65.
[19] Jansen MMM, Gracia JM, Kizilkaya AC, et al. How surface reactivity depends on the configuration of coadsorbed reactants: CO oxidation on Rh(100). J Phys Chem C. 2010;114:17127–17135.
[20] Baraldi A, Dhanak VR, Comelli G, et al. Order-disorder phase transitions of oxygen on Rh(100). Phys Rev B. 1997;56:10511–10517.
[21] Norris AG, Schedin F, Thornton G, et al. X-raysurface X-ray diffraction study of the Rh(100)(2 × 2)-O reconstruction. Phys Rev B. 2000;62:2113–2117.
[22] Saliba N, Parker DH, Koel BE. Adsorption of oxygen on Au(111) by exposure to ozone. Surf Sci. 1998;410:270–282.
[23] Livneh T, Asscher M. Photoinduced fragmentation of multilayer CH_3Br on Cu/Ru(001). J Phys Chem B. 2003;107:11382–11390.
[24] Woodruff DP, Delchar TA. Modern techniques of surface science. Cambridge Solid State Science Series, Cambridge: Cambridge University; 1986.
[25] Somorjai GA. Introduction to surface chemistry and catalysis. New York (NY): Wiley; 1994.
[26] Richter LJ, Germer TA, Ho W. Coadsorption-induced site changes: bridging hydrogen from CO and H on Rh(100). Surf Sci. 1988;195:L182–L192.
[27] Kim Y, Peebles HC, White JM. Adsorption of D2, CO and the interaction of CO-adsorbed D2 and CO on Rh(100). Surf Sci. 1982;114:363–380.
[28] Hennig D, Wilke S, Lober R, et al. The adsorption of hydrogen on Pd(100) and Rh(100) surfaces: a comparative theoretical study. Surf Sci. 1993;287:89–93.
[29] Pauer G, Eichler A, Sock M, et al. Identification of new adsorption sites of H and D on rhodium(100). J Chem Phys. 2003;119:5253–5266.
[30] Gurney BA, Richter LJ, Villarrubia JS, et al. The populations of bridge and top site CO on Rh(100) vs coverage, temperature, and during reaction with O. J Chem Phys. 1987;87:6710–6721.
[31] Jansen APJ. Monte Carlo simulations of temperature-programmed desorption spectra. Phys Rev B. 2004;69:1–6.
[32] Kose R, Brown WA, King DA. Role of lateral interactions in adsorption kinetics: CO/Rh(100). J Phys Chem B. 1999;103:8722–8725.
[33] Baraldi A, Gregoratti L, Comelli G, et al. CO adsorption and CO oxidation on Rh(100). Appl Surf Sci. 1996;99:1–8.
[34] Jansen MMM, Gracia J, Nieuwenhuys BE, et al. Interactions between co-adsorbed CO and H on a Rh(100) single crystal surface. Phys Chem Chem Phys. 2009;11:10009–10016.
[35] Hopstaken MJP. Elementary reaction kinetics and lateral interactions : in the catalytic reaction between NO and CO on rhodium surfaces [PhD thesis]. Eindhoven: Eindhoven University of Technology; 2000.
[36] Hopstaken MJP, Niemantsverdriet JW. Structure sensitivity in the CO oxidation on rhodium: effect of adsorbate coverages on oxidation kinetics on Rh(100) and Rh(111). J Chem Phys. 2000;113:5457–5465.
[37] Hopstaken MJP, Niemantsverdriet JW. Lateral interactions in the dissociation kinetics of NO on Rh(100). J Phys Chem B. 2000;104:3058–3066.
[38] Ho P, White JM. Adsorption of NO on Rh(100). Surf Sci. 1984;137:103–116.